

# FEL GAIN LENGTH AND TAPER MEASUREMENTS AT LCLS \*

D. Ratner<sup>†</sup>, A. Brachmann, F.J. Decker, Y. Ding, D. Dowell, P. Emma, J. Frisch, S. Gilevich, G. Hays, P. Hering, Z. Huang, R. Iverson, H. Loos, A. Miahnahri, H.D. Nuhn, J. Turner, J. Welch, W. White, J. Wu, D. Xiang, G. Yocky (SLAC, Menlo Park, California)  
W. M. Fawley (LBNL, Berkeley, California)

## Abstract

We present experimental studies of the gain length and saturation power level from 1.5 nm to 1.5 Å at the Linac Coherent Light Source (LCLS). By disrupting the FEL process with an orbit kick, we are able to measure the X-ray intensity as a function of undulator length. This kick method is cross-checked with the method of removing undulator sections. We also study the FEL-induced electron energy loss after saturation to determine the optimal taper of the undulator K values. The experimental results are compared to theory and simulations.

## INTRODUCTION

We present gain length measurements from LCLS, the world's first hard X-ray laser. LCLS first lased on April 10th, 2009 [1]. We measured the first gain lengths and FEL saturation four days later. In this paper we describe the methods used to measure both gain lengths and post-saturation power growth and present results from early diagnostics.

## GAIN LENGTH MEASUREMENTS

The primary diagnostic for initial gain length measurements was a YAG fluorescence screen located 50 m downstream from the last undulator. We determined X-ray power by summing pixels within a  $5\sigma$  region of interest around the FEL spot. We also compared the simple summing analysis to various fitting methods and observed little difference. Two neutral density filters with a total transmission of 0.01% extended the camera's dynamic range to more than 4 orders of magnitude.

More recently, LCLS has switched to a new set of diagnostics in the Front End Enclosure (FEE). These include additional YAG screens and cameras, two gas detectors, a total energy monitor and a suite of solid and gas X-ray attenuators that will prevent YAG saturation. Future data will be taken with the FEE diagnostics.

### Undulator Removal Method

To determine the FEL gain length, we must measure the FEL power as a function of position along the undulator. Due to practical considerations, the power diagnostics follow the final undulator. Consequently, to determine power

as a function of position, we must disrupt the FEL process. With 3.35 m long undulator segments and soft X-ray gain lengths as short as 1.5 m, we would ideally measure the power following each undulator segment. The most direct method for suppressing the FEL is to sequentially remove undulators, with the added benefit of a decreased spontaneous background signal, which helps low FEL power measurements. However, each undulator requires 3 minutes to remove (more than 90 minutes for a full  $P(z)$  scan), so initial concerns about the temporal FEL stability prompted interest in an alternative method.

### Transverse Kick Method

Rather than removing undulators, we can instead disrupt the FEL process. For example, introducing a distortion to the electron orbit suppresses the FEL by decreasing bunching and beam overlap [2] (Fig. 1). By kicking the beam transversely at sequential positions in the undulator hall, we can measure the FEL gain length.

Following each LCLS undulator, a pair of  $x$  and  $y$  dipole correctors can kick the beam by approximately  $15\ \mu\text{radians}$  in each plane. The requirement for FEL suppression is determined by the critical angle,  $\phi_c = \sqrt{\lambda_R/L_G}$ , with FEL wavelength  $\lambda_R$  and gain length,  $L_G$ . For hard X-rays at LCLS,  $\phi_c \approx 7\ \mu\text{radians}$ , so the dipole correctors can strongly suppress the FEL process in the downstream undulators. The kick method is less effective at longer wavelengths, when the critical angle is much larger and the beta function is smaller. Using the kick method, a full  $P(z)$  scan can be completed in under 10 minutes. We show good agreement between the two methods at 1.5 Å in Fig. 2.

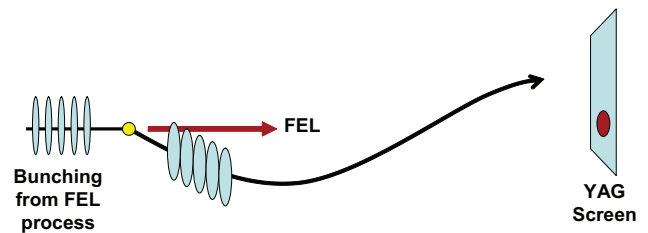


Figure 1: After a transverse dipole kick, the FEL process is suppressed.

### Restarting FEL with Kick Method

Though the kick method is faster and generally equivalent in accuracy to the undulator removal method, we do

\* Work supported by Department of Energy contracts DE-AC02-76SF00515 and DE-AC02-05CH11231

<sup>†</sup> dratner@slac.stanford.edu

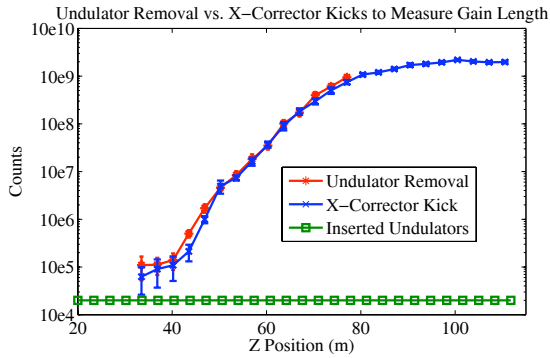


Figure 2: Gain lengths measured with both the undulator removal and dipole corrector kick methods. Distances are for total undulator length and do not include the breaks between segments.

note some drawbacks. First, the background signal at low power (when the beam is kicked early) is larger than in the undulator removal method, where the spontaneous background is proportional to the number of inserted undulators. Second, distorting the orbit near the beginning of the undulator hall may allow the FEL process to restart, leading to secondary (though weak) FEL spots (Fig. 3). We observe restart occurring in two places: after a  $\pi/2$  phase advance and further downstream when the orbit distortion straightens (Fig. 4). An additional kick further down the undulator (for instance at slightly more than a  $\pi/2$  phase advance) effectively suppresses both secondary spots. Given the spatial separation of the spots (as seen in the cartoon, Fig. 4), an alternative solution is to select a sufficiently small region of interest around the primary FEL.

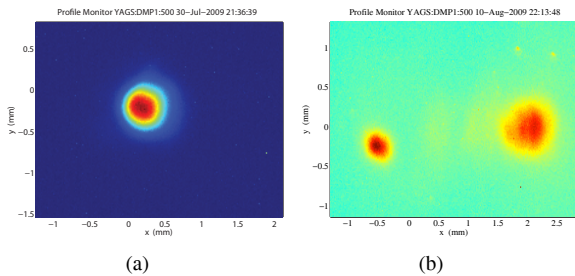


Figure 3: At left, the primary FEL spot at saturation is centered around 0.25 mm. At right, after strongly suppressing the main FEL peak (faintly visible around  $x \approx 0.5$  mm), secondary FEL spots emerge on either side (though several orders of magnitude weaker than the saturated primary FEL). The left-hand secondary spot emerges from the straight section of the orbit distortion.

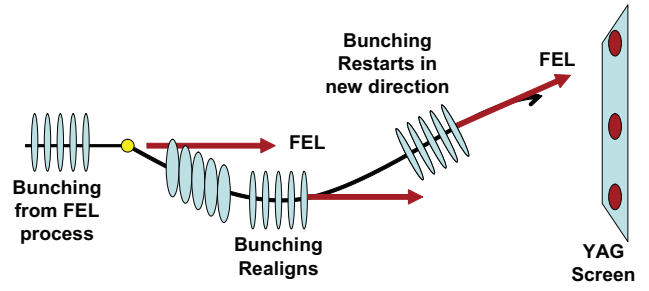


Figure 4: The bunching can either realign or restart from shot noise, creating secondary FEL spots. In this cartoon, down corresponds to positive X on the YAG screen

## RESULTS

### LCLS Gain Length

Due to the danger of damaging the YAG screen at low energies, we have primarily studied the gain length at 1.5 Å radiation (13.6 GeV electron beam). After optimizing the electron beam parameters we have measured gain lengths as short as  $2.85 \pm 0.06$  m at 250 pC (Fig. 5). More typically, we measure gain lengths between 3 and 4 m, which agree with Genesis [4] simulation results for a beam with  $0.4 \mu\text{m}$  normalized emittance (Fig. 6). The shortest gain lengths may be due to sections of the beam having even lower emittance or from lasing in the wake-field induced current spikes (Fig. 7).

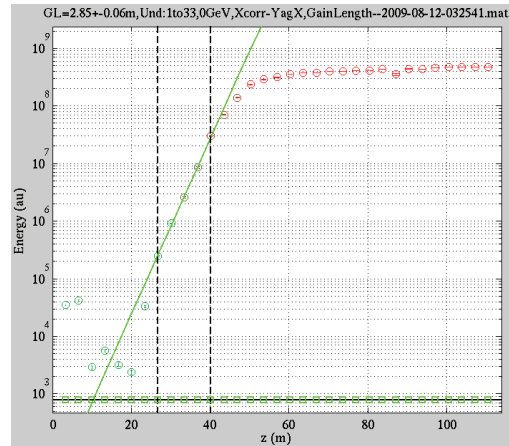


Figure 5: Gain length of  $2.85 \pm 0.06$  m taken at 13.6 GeV using the dipole corrector method. The high power levels of the first two data points are due to a secondary FEL spot as seen in Fig. 3.

To measure gain lengths at 1.5 nm wavelength, we remove all but 9 undulators to reduce the overall power hitting the YAG screen. The FEL is harder to suppress at longer wavelength; secondary FEL spots reflect off the beam pipe and interfere with the corrector kick measurements. The undulator removal method is slow, but remains effective at all wavelengths. We measure a gain length of

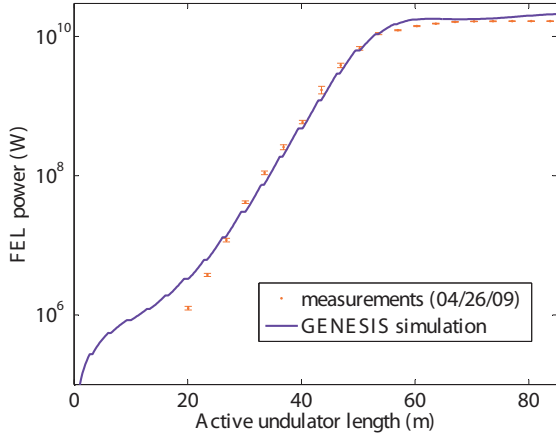


Figure 6: A gain length measurement of 3.3 m agrees well with Genesis simulations for a beam with  $0.4 \mu\text{m}$  emittance.

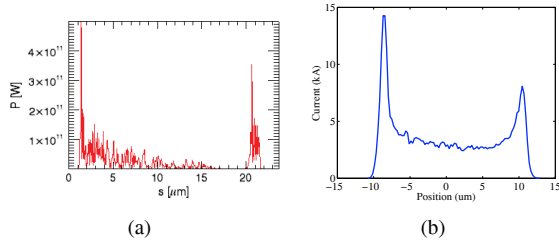


Figure 7: Genesis simulation showing power as a function of longitudinal bunch position (left). The peak power occurs in the current spikes (right). For this simulation, the spikes had emittances of  $0.6 \mu\text{m}$ .

$1.62 \pm 0.15 \text{ m}$  at 4.7 GeV beam energy (Fig. 8).

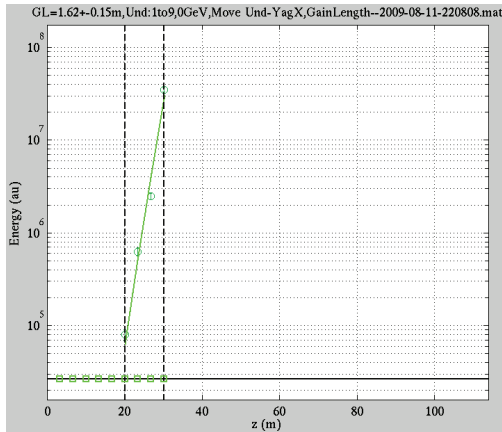


Figure 8: Gain length of  $1.62 \pm 0.15 \text{ m}$  taken at 4.7 GeV using the undulator pull method.

### Gain Length vs. Energy Spread

With the kick method taking less than 10 minutes for a full  $P(z)$  scan, we can measure gain length as a func-

tion of various electron beam parameters. In Fig. 9 we show one example: gain length vs. laser-heater induced energy spread. The laser heater increases the energy spread by  $\Delta E \approx 8\sqrt{P_L}$ , with the laser heater energy,  $P_L$ , in mJ [3]. The final energy spread is then multiplied by the bunch compression factor,  $\sim 90$  at 3 kA. The results are consistent with the Xie scaling [5] for  $0.4 - 0.5 \mu\text{m}$  beam emittance. We also note that the gain length with the laser heater off (0 keV) is approximately 1 m higher than at the nominal heater value (20 keV). We attribute the increased gain length in the case of no laser heating to self-heating from the microbunching instability [7].

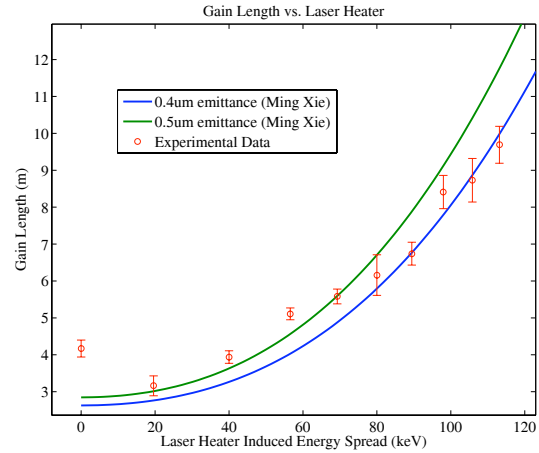


Figure 9: Gain length as a function of energy spread following the laser heater. Ming Xie scaling shown for  $0.4, 0.5 \mu\text{m}$  emittances. We note the increased gain length with no laser heating (0 keV), hinting at the importance of the laser heater to suppress the microbunching instability. The nominal heater value induces a 20 keV energy spread.

### Saturation Taper

Tapering the undulator K parameter near and beyond saturation can increase the final FEL power [8, 9]. As the electrons lose energy to the radiation field, the resonance condition moves towards longer wavelengths. Changing the K value compensates for energy loss and keeps the resonance condition fixed. Longitudinal wakefields and incoherent spontaneous emission losses require use of a linear  $K(z)$  taper across all undulators; the necessary slope can be calculated from electron beam parameters. To compensate for additional FEL-induced energy loss, we empirically scanned linear saturation tapers, changing both the slope and starting point, to find the optimal K values (Fig. 10).

To evaluate our taper we use the same dipole corrector kick method as was used for the gain length studies. The YAG screen saturates before the FEL does, so we must infer the FEL power from the average electron energy loss, measured with BPMs in the electron dump. The

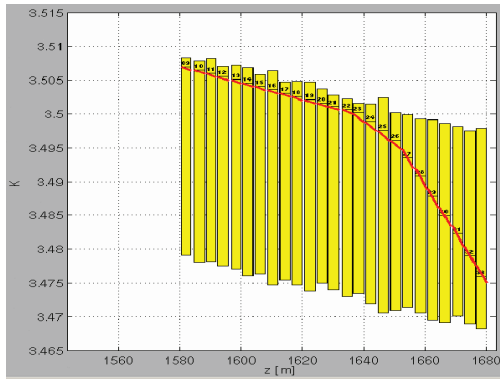


Figure 10: Experimentally-optimized undulator taper (red line) that yielded an FEL-induced average electron energy loss of nearly 9 MeV. Yellow boxes show available range of taper for each undulator.

kick method does not affect either spontaneous radiation or wakefields; consequently, any change in energy loss that correlates to a transverse kick must result from the FEL. The FEL-induced energy loss before saturation is small relative to the measurement noise, so this method is not effective for measuring the gain length.

Results from one such taper measurement, along with Genesis simulations of the same LCLS parameters, are shown in Fig. 11. We can also compare the power gain relative to the untapered case (Figs. 12, 13). Experimentally we observe a gain factor of 2.4, somewhat smaller than the factor of 3.3 found in Genesis simulations.

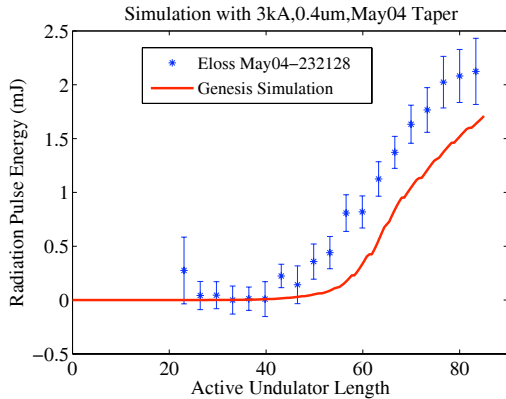


Figure 11: Post-saturation FEL pulse energy for a taper with nearly 9 MeV final average electron energy loss. Genesis simulations for a  $0.4\mu\text{m}$  emittance beam agree well, but have slightly less FEL power.

## CONCLUSION

We have presented the first gain length and taper measurements from LCLS. We find gain lengths of  $\sim 2.9 - 3.3$  at  $\lambda_R = 1.5 \text{ \AA}$ , and 1.65 m at  $\lambda_R = 1.5 \text{ nm}$ . We also can more than double the coherent, FEL power over the satura-

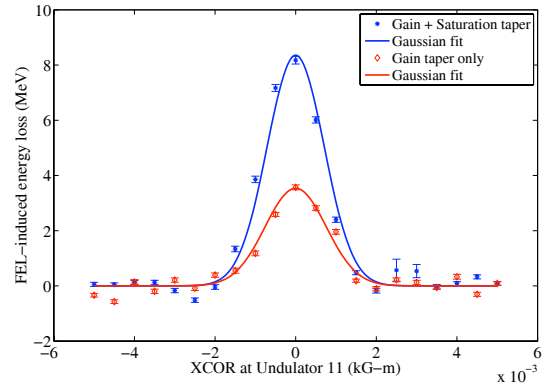


Figure 12: Measured FEL-induced electron energy loss as a function of dipole kick at undulator 11. The addition of a saturation taper can increase the FEL output by a factor of greater than 2.

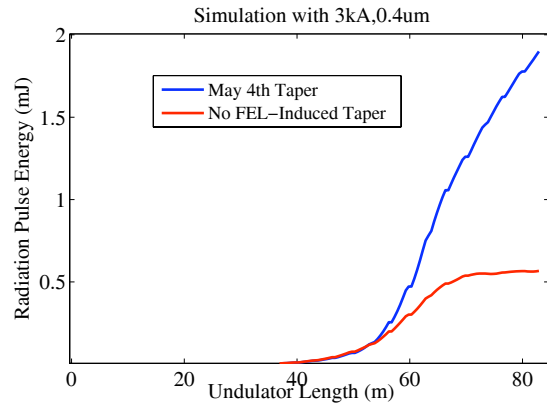


Figure 13: Simulation results show a post-saturation taper increasing the FEL output by greater than a factor of 3.

tion value by tapering the downstream undulators.

## REFERENCES

- [1] P. Emma, et al., First Lasing of the LCLS X-Ray FEL at 1.5  $\text{\AA}$ , Proceedings of PAC '09.
- [2] T. Tanaka, H. Kitamura, and T. Shintake, Nucl. Instrum. Methods Phys. Res., Sect. A **528**, 172 (2004).
- [3] P. Emma, *et al.*, First Results of the LCLS Laser-Heater System, Proceedings of PAC '09.
- [4] S. Reiche, Nucl. Instrum. Meth. A **429**, 243 (1999).
- [5] M. Xie, Proceedings of PAC 95 and IUPAP, pp 183-185.
- [6] M. Xie, Nucl. Instrum. Methods Phys. Res., Sect. A **445**, 59 (2000).
- [7] Z. Huang, M. Borland, P. Emma, J. Wu, C. Limborg, G. Stupakov and J. Welch, Phys. Rev. ST Accel. Beams **7**, 074401 (2004).
- [8] N. M. Kroll, P. L. Morton and M. N. Rosenbluth, IEEE J. Quant. Electron. **17**, 1436 (1981).
- [9] W.M. Fawley *et al.*, Nucl. Instrum. Methods Phys. Res. A **483** 537 (2002).